Development of a high performance donor-acceptor conjugated polymer – synergy in materials and device optimization

Mei Gao,[†]* Jegadesan Subbiah,[‡] Paul B. Geraghty,[‡] Ming Chen,[†] Balaji Purushothaman,[‡] Xiwen Chen,[†] Tianshi Qin,[†] Doojin Vak,[†] Fiona H. Scholes,[†] Scott E. Watkins,[†] Melissa Skidmore,[†] Gerard J. Wilson,[†] Andrew B. Holmes,[‡] David J. Jones,[‡]* Wallace W. H. Wong[‡]*

CSIRO Manufacturing Flagship, Bag 10, Clayton South, Victoria 3169.

School of Chemistry, Bio21 Institute, University of Melbourne, 30 Flemington Road, Victoria 3010, Australia.

E-mail: Mei.Gao@csiro.au, djjones@unimelb.edu.au, wwhwong@unimelb.edu.au

ABSTRACT: The development of a high performance polymer **PBDT-BT** for bulk heterojunction solar cell devices is summarized. The polymer was first synthesized by Stille polycondensation and solar cell devices in conventional geometry was optimized through the use of a lithium salt cathode interlayer reaching 6% power conversion efficiency. Improvements were made to the synthesis of the polymer using Suzuki polycondensation giving high molecular weight material in the Mn 100 kg/mol range. Further device optimization in inverted geometry gave power conversion efficiency of over 9%. The synthesis scalability as well as the batch-to-batch reproducibility of the polymer were extensively investigated.

Introduction

In the last decade, the development of polymer solar cells has been driven by research in chemistry, physics and engineering making it a truly interdisciplinary topic. The various performance benchmarks could not have been achieved without the close collaboration of synthetic chemists, physical chemists, device physicists and engineers. In a bid to demonstrate the possibility of printing large area flexible polymer solar cells with good performance and stability, our team embarked on a project that involved the development of new materials, device architecture, printing processes and device encapsulation. In this article, we report the material and device optimization of a donor-acceptor conjugated polymer system which cumulated in the publication of high performance bulk heterojunction (BHJ) solar cell devices of over 9% power conversion efficiency (PCE).[1] This work was performed over a period of several years with contributions from a substantial number of researchers working in various relevant scientific disciplines. A number of new results are included in this paper – 1. A solution processable lithium salt interlayer was used in a polymer solar cell for the first time; 2. The rapid synthesis of the polymer was demonstrated in flow processing and; 3. Batch to batch polymer variation was investigated in relation to their device performance. It is envisaged that this report will serve as a guide not only for the development of polymer solar cells but organic electronic devices in general.

Materials Design

The initial part of our printed solar cell research program relied on materials that are available in substantial quantities.[2, 3] As such, poly(3-hexylthiophene) P3HT and phenyl-C_{61}-butyric acid methyl ester ($PC_{61}BM$) were the photoactive material combination of choice. However, that system has limited performance in devices. In order to quickly develop higher performance in-house materials, reported literature was used extensively to guide the design of materials.[4] In particular, benzodithiophene (BDT) based donor-acceptor conjugated polymers were proving very popular with numerous examples showing impressive performance.[5-7] Structural variations were made to tune the photophysical properties, such as spectral coverage and absorptivity, as well as solution processability, crystallinity and charge transport properties. When considering the design of materials for large area printed devices, the essential criteria are material availability and solution processability.[8] Therefore, we aimed to keep the polymer backbone structure as simple as possible with side chain variations to tune solubility (Figure 1). Once the promising structure was identified, most of our research effort was directed towards the optimization of the polymerization process (*vide infra*).

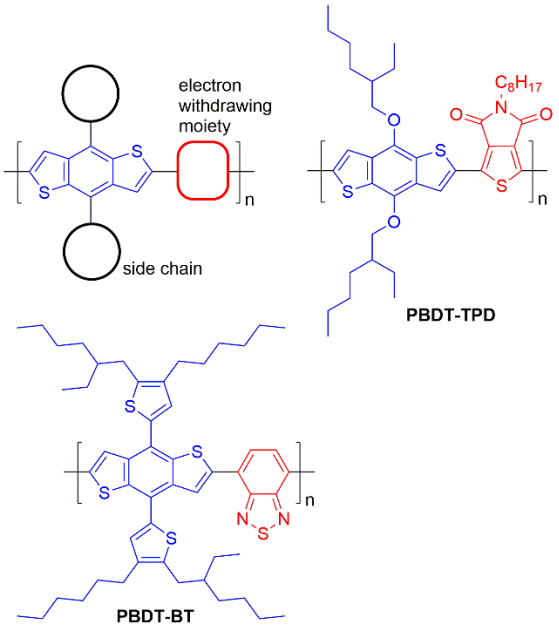

Figure 1. Chemical structure illustrations of high performance polymer **PBDT-BT** developed in this work and commercially available polymer **PBDT-TPD**.

Device Structure

Optimization of device structure and fabrication process must be performed to achieve high performance solar cells. A common approach is to use a standard set of fabrication conditions and device structure to screen materials. This ensures higher throughput testing and feedback to improve material design. A set of materials property parameters, such as spectral absorption range and intensity, frontier orbital energy levels and solution processability, was used to identify promising materials.[9] Once a candidate was chosen, maximum performance of the material can be extracted through device optimization. Device optimization is a multi-component problem. Basic variations include polymer-fullerene blend ratio, film thickness, processing solvent, the use of additives and post-deposition annealing. These parameters have significant effects on the nanostructure of the active layer films.[10] Ideal nanostructure means high efficiency of exciton separation and transport of charges towards the electrodes. The extraction of charges from the active layer to the electrodes can be improved by using interlayer materials.[11-14] Interlayers can enhance both physical and electronic contact between the active layer and the electrodes. Once the overall efficiency has been optimized, the stability of devices has to be considered. It has been well established that devices fabricated with inverted geometry are much more stable than ones in conventional geometry. However, different active layer material combinations can have varying performance when used in these device geometries. In this study, a range of device optimization methods were employed to increase the PCE of polymer solar cells containing **PBDT-BT** from 2% to over 9%.

Results and Discussion

As indicated in the introduction, the development of materials and devices presented in the sections below occurred over a significant time period with a number of researchers involved. The description of the work has been divided into two parts. The initial phase is material design and device testing to screen materials. The second phase is materials synthesis and device optimization.

First Generation Materials and Devices

At the start of the development on BDT-based polymeric materials, a few examples stood out with their good device performance.[6] The chemical structure of one example, **PBDT-TPD**, is shown in Figure 1.[15-17] As the priority of the project was to obtain high performance in-house materials as quickly as possible, we set about making easily interchangeable variation with the acceptor building block of the polymer and adding side chains to ensure solution processability. A series of polymers were synthesized and tested in devices with some examples published.[18-22] In this article, the focus is on the optimization of the benzodithiophene-benzothiadiazole copolymer, **PBDT-BT**.[1]

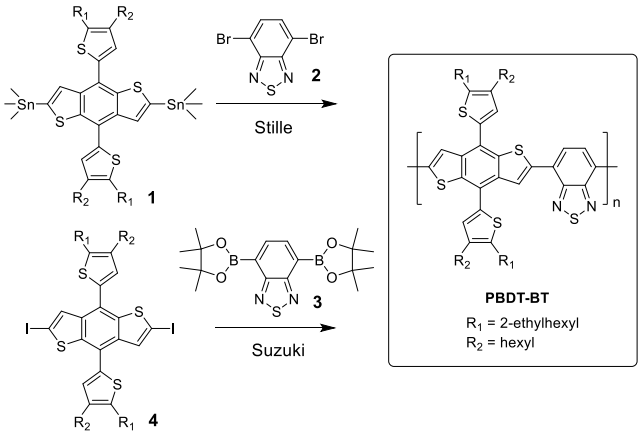

Figure 2. Synthesis of **PBDT-BT** via Stille and Suzuki polycondensation.

PBDT-BT was first synthesized by Stille coupling between the BDT bis-tin compound **1** and dibromobenzothiadiazole **2** (Figure 2, see Supporting Information for details). While polymeric material of reasonable molecular weight was obtained from this reaction, reproducibility was a problem with batch to batch molecular weight variations. It was found that small scale polymerizations using highly purified BDT **1** gave substantially high molecular weight material compared to large batches. The stability of the BDT monomer **1** was such that recycling gel permeation chromatography (GPC) was the only purification method capable of delivering high purity material.[22] However, the scalability of this method was severely limited. Full characterization of the polymer was obtained from a larger scale synthesis which was also

used in the initial device testing and optimizations (see Supporting Information). The molecular weight of this polymer batch was found to 17 kg/mol number average (M_n) with polydispersity index (PDI) of 2.4 in high temperature GPC measurements against narrow polystyrene standards.

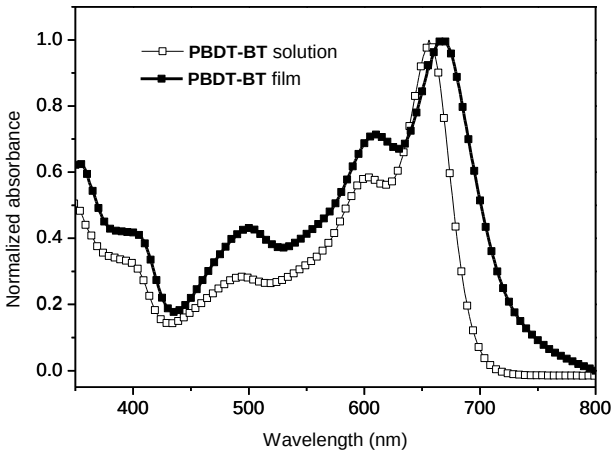

Figure 3. Normalized UV-Vis absorption spectrum of **PBDT-BT** in chloroform solution and in thin film.

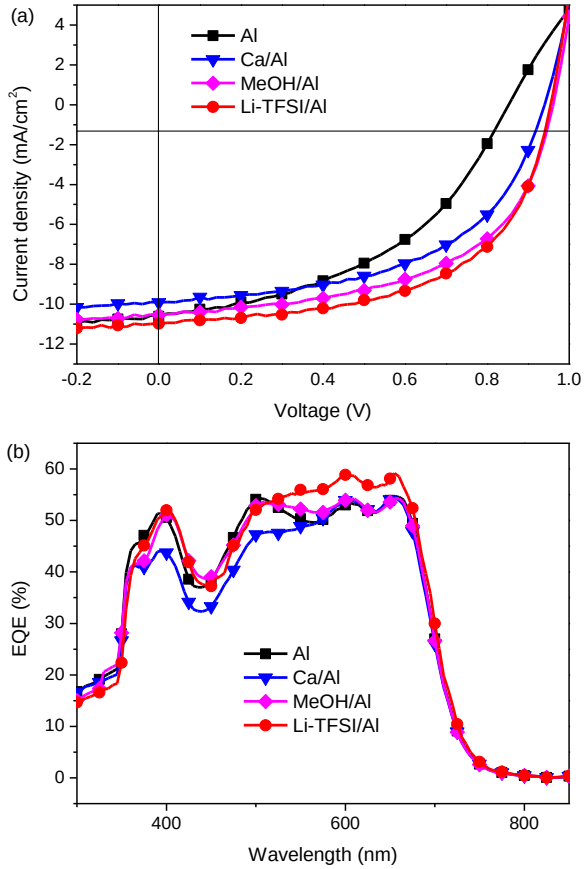

Figure 4. (a) Current density vs. voltage curves and (b) photo-response data for devices containing **PBDT-BT** with various cathode layers.

The decomposition temperature (5% weight loss from thermal gravimetric analysis) for polymer fractions was at ca. 420 °C and no thermal phase transitions were detected in differential scanning calorimetry. The UV-Vis absorption maximum for the polymer was 650 nm in solution and 660 nm in film (Figure 3) while the photoluminescence maximum was 690 nm. The highest occupied molecular orbital (HOMO) energy was measured using both electrochemical experiments (-5.43 eV) and the photo-electron spectroscopy in air technique (-5.29). It is important to note that these basic polymer characterization data was essentially identical for all polymer samples with different molecular weights and synthesized using different methods (*vide infra*, see Supporting Information, Table S2).

Despite the synthesis issues, the **PBDT-BT** material was tested in devices giving promising results. Initial device optimization included film thickness and polymer-fullerene blend ratio (Table 1, entry 1-3). A **PBDT-BT**:$PC_{61}BM$ weight ratio of 1:1.5 was found to be optimum with PCE of 4.5% recorded. The films were deposited by spin coating from chlorobenzene solution (37.5 mg/mL). The basic device geometry used for materials screening in our laboratories was ITO/PEDOT:PSS/active layer/Al. To further improve device performance, a variety of cathode interlayer treatments were examined.[11, 23, 24]

Solution processed interlayer materials were particularly attractive for our program as the ultimate goal was to fabricate large area devices using roll-to-roll printing.[3] Vacuum deposited calcium, a commonly employed cathode interlayer material, was compared with the solution processable bis(trifluoromethane)sulfonimide lithium salt (Li-TFSI). Li-TFSI has been used extensively as an additive in solid state dye sensitized solar cells to promote the doping of the solid state electrolyte.[25, 26] As the Li-TFSI was deposited from methanol solution, devices simply treated with methanol were also tested as methanol has been shown to enhance performance.[23] A summary of device performance results are presented in Table 1. To show the applicability of the Li-TFSI layer, devices were prepared with a commercially available polymer, **PBDT-TPD**. It is noteworthy that the optimal concentration of the Li-TFSI solution was 5 mg/mL spin coated at 5000 rpm leading to extremely thin coatings.

The device performance improvements with the use of Li-TFSI was significant (Table 1 and Figure 4). As expected, increase in open circuit voltage (V_{oc}) was observed for all interlayer treatments compared to the use of Al only.[11] It was also encouraging to observe increase in short circuit current density (J_{sc}) and fill factor (FF) when comparing the Li-TFSI with Ca and methanol. This was true for both **PBDT-BT** and **PBDT-TPD** polymer systems. The interlayers substantially lowered the sheet resistance (R_s) of the devices and improved the shunt resistance (R_{sh}). The maximum PCE was recorded for devices containing

Table 1. Device data for solar cells containing **PBDT-BT** (M_n 17 kg/mol) synthesized by Stille polycondensation and **PBDT-TPD** in conventional device geometry.

Entry	Device geometry	V_{oc} V	J_{sc} [a] mA/cm^2	FF %	PCE [b] %	R_s Ωcm^2	R_{sh} Ωcm^2
1	ITO/PEDOT:PSS/**PBDT-BT**:$PC_{61}BM$ (1:1)/Al	0.74	6.82	45	2.25 (2.15 ±0.12)	27	230
2	ITO/PEDOT:PSS/**PBDT-BT**:$PC_{61}BM$ (1:2)/Al	0.84	10.68 (10.37)	46	4.13 (3.93 ±0.20)	25	340
3	ITO/PEDOT:PSS/**PBDT-BT**:$PC_{61}BM$ (1:1.5)/Al	0.86	10.41 (10.31)	50	4.48 (4.28 ±0.09)	22	480
4	ITO/PEDOT:PSS/**PBDT-BT**:$PC_{61}BM$ (1:1.5)/Ca/Al	0.94	9.92 (9.72)	53	4.96 (4.76 ±0.10)	17	650
5	ITO/PEDOT:PSS/**PBDT-BT**:$PC_{61}BM$ (1:1.5)/MeOH/Al	0.96	10.39 (10.24)	55	5.60 (5.42 ±0.15)	14	590
6	ITO/PEDOT:PSS/**PBDT-BT**:$PC_{61}BM$ (1:1.5)/Li-TFSI/Al	0.96	10.98 (10.54)	57	5.97 (5.60 ±0.19)	11	630
7	ITO/PEDOT:PSS/**PBDT-TPD**:$PC_{61}BM$ (1:1.5)/Al	0.74	9.47 (9.04)	55	3.52 (3.28 ±0.10)	16	580
8	ITO/PEDOT:PSS/**PBDT-TPD**:$PC_{61}BM$ (1:1.5)/Ca/Al	0.82	9.52	58	4.54 (4.30 ±0.15)	10	600
9	ITO/PEDOT:PSS/**PBDT-TPD**:$PC_{61}BM$ (1:1.5)/MeOH/Al	0.92	9.59 (9.41)	57	5.07 (5.03 ±0.02)	12	610
10	ITO/PEDOT:PSS/**PBDT-TPD**:$PC_{61}BM$ (1:1.5)/Li-TFSI/Al	0.94	10.00 (9.92)	62	5.80 (5.51 ±0.24)	9	790

[a] Current density calculated from EQE data in brackets; [b] Device performance are from the best devices with average PCE values based on 12 devices shown in brackets.

the Li-TFSI interlayer for both **PBDT-BT** and **PBDT-TPD** polymer systems at 5.97% and 5.80% respectively (Table 1, entry 6 and 10). The spectral response of the devices showed that higher external quantum efficiency (EQE) was observed in the 500 nm to 700 nm region with Li-TFSI interlayer (Figure 4b). This corresponded to the improved current output of those devices. While the device performance improvement is not very large going from methanol treated to Li-TFSI treated devices, there is a statistical difference (Table 1, entries 5-6 and 9-10).

The active layer film surface was examined to ascertain the effect of the Li-TFSI treatment. X-ray photoelectron spectroscopy showed the presence of lithium and fluorine atoms on the polymer film surface (Figure S14). Atomic force microscopy (AFM) images of the polymer surface before and after Li-TFSI treatment were very similar (Figure S12). The treatment did not have significant effects on the surface structure of the polymer films which meant that the device improvements could be attributed to electronic effects of the Li salt. The solution deposition of Li-TFSI is convenient and low-cost and should be widely applicable as the cathode interlayer in BHJ devices with conventional geometry.

Materials Synthesis and Device Optimization

At the time of the study, materials that showed 6% PCE in devices were considered a significant benchmark. In fact, the HOMO and LUMO energy of the **PBDT-BT** polymer was -5.45 eV and -3.7 eV respectively. Some theoretical estimates for solar cell device performance have indicated potential PCE of ~8% for a donor material with these energy level values.[9] With an in-house material of good performance, the next target was to produce larger quantities of the **PBDT-BT** material and use it in our printed solar cell program. As mentioned in the previous section, the Stille polycondensation method was not very reliable especially at large scale. In addition, the demands of roll-to-roll printing meant that 10's to 100's of gram quantities had to be considered. Parallel to the materials and device development program, our group was working on alternative synthesis techniques to overcome scale-up issues. We demonstrated that it was possible to synthesize a variety of organic electronic materials, including conjugated polymers, using continuous flow methods.[27-31] Related examples of conjugated polymer synthesis in continuous flow has also been demonstrated by others in the literature.[32, 33]

At first, Stille polycondensation in flow to produce **PBDT-BT** was examined. It was quickly found that the solubility of the dibromobenzothiadiazole **2** was not compatible with the flow process. The polymerization reaction occurred most efficiently at monomer concentrations of at least 0.1 M but compound **2** did not have that level of solubility in toluene. While this was not an issue in conventional batch reactions, reagents had to be fully dissolved to enable unobstructed flow through the pumping mechanism of the flow synthesis equipment.[27, 30] As such, there were two very good reasons to redesign the synthesis – 1. solubility of reagents and 2. avoid the use of organotin monomer **1** which had stability issues and was difficult to purify.

The use of Suzuki polycondensation solved the problems associated with the Stille reaction (Figure 2). The solubility of the benzothiadiazole building block was greatly improved when functionalized with boronic acid pinacol esters required for Suzuki coupling. In addition, both the boronic acid pinacol ester compound **3** and the diiodo-BDT monomer **4** were easily purify by recrystallization. It was noteworthy that diiodo monomer **4** was used instead of the more commonly observed arylbromide compounds in Suzuki polycondensations. The bromination of the BDT core had significant regioselectivity issues in attempts to obtain the dibromo analogue of **4** via a number of synthetic approaches, such as bromination with N-bromosuccinimde. Lithiation and iodination gave high purity monomer **4** after column chromatography and recrystallization.

With significant quantities of pure monomers for Suzuki coupling, the polymerization was examined in both conventional and flow conditions. Biphasic Suzuki reaction conditions (toluene/water) were investigated with a number of palladium catalyst and base combinations. The most reactive combination was found to be tris(dibenzylideneacetone)-dipalladium(0) with tris(*o*-tolyl)phosphine as the catalyst species and aqueous carbonate as base. A phase transfer reagent was required and Aliquat 336 was used initially. The rate of polymerization was surprisingly fast. Formation of a dark blue polymer gel was observed in less than 30 min when the reaction was heated at up to 100 °C. Analysis of the molecular weight of these polymer batches were found to be extremely high with one measurement recorded with weight average (M_w) of 3700 kg/mol. Given the solubility of the polymers, the accuracy of the molecular weight numbers could be questioned but it was still an indication of polymerization rate. Clearly, it was necessary to have better control over the reaction.

With 0.2 M monomer concentration and reaction temperature of 65 °C, gelation of the reaction mixture was observed after 1 h and polymeric material was isolated by solvent extraction after a further hour of heating and end capping (see Supporting Information for details). A typical batch reaction performed under those conditions would result in four solvent extracted fractions – dichloromethane (DCM), chloroform (CF), toluene (Tol) and chlorobenzene (CB). These fractions were thoroughly examined in our previous communication and the Tol fraction with M_n of 112 kg/mol showed a maximum performance of 9.4% PCE.[1] A discussion on the device optimization is provided after the synthesis discussions below.

Armed with a good knowledge of the reactivity in conventional batch synthesis, flow synthesis of **PBDT-BT** was investigated (Figure 5). Keeping the monomer concentration at 0.1 M and 4 mol% Pd catalyst, variations on residence time and temperature were tested (see Supporting Information for details). From the results, it was apparent that Suzuki polycondensation in flow could not achieve the molecular weight ranges obtained in batch reaction but was still superior to the molecular weight of material from batch Stille polycondensations (Table 2). Directly sampled from the reaction mixtures, M_n as high as 73 kg/mol was recorded (Table 2, entry 7). Toluene extracts gave values of 43 kg/mol and 101 kg/mol for M_n and M_w respectively. The most interesting aspect of the flow polymerizations was that reactions heated at 130 °C reached maximum molecular weight after 5 min. Such short reaction times for conjugated polymers is highly unusual with the majority of literature Stille and Suzuki polycondensations requiring several hours to several days.[30]

Despite the relatively successful outcome of the flow reactions, significant quantities of the high performance **PBDT-BT** material (i.e. the toluene extract) could only be obtained by conventional batch processing. Further complicating our efforts was the fact that scaling up the batch reactions did not produce polymeric material with reliable molecular weight distributions. For example with monomer concentration at 0.2 M, a 5-mL reaction would give a different

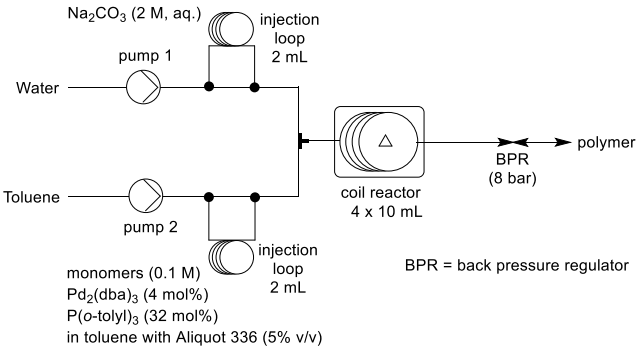

Figure 5. Continuous flow setup for the synthesis of **PBDT-BT** via Suzuki coupling.

Table 2. Reaction conditions and molecular weight outcome for **PBDT-BT**.

Entry	Setup	Temp °C	Time min	M_n kg/mol	PDI
1	Stille [a]	170	60	17	2.4
2	Suzuki batch [b]	30	120	28	2.5
3	Suzuki batch [b]	40	120	124	3.6
4	Suzuki batch [b]	60	60	151	5.8
5	Suzuki flow [c]	90	100	15	3.5
6	Suzuki flow [c]	120	20	20	2.4
7	Suzuki flow [c]	130	5	73	2.7

Note that molecular weight data in this table (except for entry 1) was obtained from crude polymer directly sampled from the reaction without extraction. [a] Stille reaction performed with microwave heating in *o*-xylene. [b] Suzuki coupling tested in conventional batch reaction using the same reagents as in flow. [c] Continuous flow synthesis conditions described in Figure 5.

distribution of polymers to a 20-mL reaction. It was found that the onset of high viscosity in the reaction mixture as the polymers formed severely affected the mixing of the biphasic reaction. In fact, the reaction was so sensitive that reaction vessel size, stirrer bar size, stirring speed and small fluctuations in reaction temperature had some impact on the molecular weight outcome. Further investigations and modifications were made to target the prime **PBDT-BT** material with improved yield and reproducibility. It was important to note that numerous polymer batches were synthesized by this stage of the development along with their device performance parameters (Table 4). It was clear that the prime **PBDT-BT** material should have M_n of ~100 kg/mol and polydispersity of 3 to 5 in order to achieve devices with >9% PCE. Polymeric material with molecular weight lower and higher than this optimum range showed substantially lower device performance (Table 3).

Table 3. Performance parameters for devices with inverted geometry, ITO/ZnO/active layer/MoO_3/Ag.

Entry [a]	Active layer	M_n kg/mol	V_{oc} V	J_{sc} [b] mA/cm^2	FF %	PCE [c] %
1	PBDT-BT(Stille):$PC_{61}BM$ (1:2)	17	0.94	8.6	59	4.8 (4.5 ±0.3)
2	PBDT-BT(Stille):$PC_{71}BM$ (1:2)	17	0.92	9.5	60	5.3 (5.0 ±0.3)
3	PBDT-BT(DCM):$PC_{71}BM$ (1:2)	19	0.92	9.4 (9.0)	49	4.6 (4.2 ±0.2)
4	PBDT-BT(CF):$PC_{71}BM$ (1:2)	78	0.92	13.9 (13.2)	59	7.8 (7.6 ±0.3)
5	PBDT-BT(Tol):$PC_{71}BM$ (1:2)	112	0.92	14.9 (14.4)	62	8.5 (8.3 ±0.3)
6	PBDT-BT(CB):$PC_{71}BM$ (1:2)	136	0.92	13.1 (12.7)	53	6.8 (6.5 ±0.3)

[a] Data in entries 3-6 were shown in our previous communication[1]; [b] Current density calculated from EQE data in brackets; [c] Average PCE values based on 12 devices shown in brackets.

Table 4. Device performance of toluene fractions from various batches of synthesis with interlayer optimization.[a]

Entry	M_n/M_w kg/mol	Interlayer	V_{oc} V	J_{sc} mA/cm^2	FF %	PCE %
1	75/281	ZnO	0.92	12.7	63	7.3 (7.2 ±0.2)
		ZnO/PCBE-OH	0.92	13.5	66	8.2 (8.0 ±0.2)
2	88/442	ZnO	0.92	14.1	65	8.4 (8.2 ±0.2)
		ZnO/PCBE-OH	0.92	15.1	67	9.3 (9.0 ±0.3)
3	96/437	ZnO	0.92	14.2	63	8.2 (8.0 ±0.3)
		ZnO/PCBE-OH	0.92	15.0	65	9.0 (8.8 ±0.2)
4	102/509	ZnO	0.92	14.9	62	8.5 (8.3 ±0.3)
		ZnO/PCBE-OH	0.92	15.7	66	9.5 (9.2 ±0.3)
5	104/349	ZnO	0.92	16.0	57	8.4 (8.2 ±0.3)
		ZnO/PCBE-OH	0.92	16.7	60	9.2 (8.9 ±0.2)
6	108/474	ZnO	0.92	14.2	63	8.3 (8.2 ±0.2)
		ZnO/PCBE-OH	0.92	15.0	66	9.1 (8.9 ±0.3)
7	112/469	ZnO	0.92	14.5	64	8.5 (8.4 ±0.2)
		ZnO/PCBE-OH	0.92	15.4	66	9.4 (9.2 ±0.2)

[a] Device performance are from the best devices with average PCE values based on 12 devices shown in brackets. Information on the PCBE-OH interlayer can be found in the literature.[1, 20]

The Suzuki Pd catalyst system was revisited along with reaction solvent and phase transfer reagent (Table S1). Sampling a wider range of Pd sources and ligands as well as recrystallization of the catalyst species largely did not improve on the first generation optimization. The molecular weight outcome of polymerization was significantly affected by the use of different reaction solvents. Solvents, such as cyclohexane, methylcyclohexane and mesitylene, were tested to try and reduce the amount of ultra-high molecular weight chlorobenzene-soluble polymer fraction. Unfortunately, these solvents did not improve on the yield of the desired toluene-soluble fraction. Attempts were made to control the molecular weight by adjusting monomer ratios as well as adding end capping reagents. The bromo analogue of BDT monomer **4** was also tested to observe the effect of lowering the monomer reactivity. These experiments were largely unsuccessful in improving the quantity of the prime molecular weight material for devices (see Supporting Information). Lastly, phase transfer reagent, Aliquat 336, was replaced with tetradecyltrimethylammonium bromide (TTAB) to improve mixing between the organic and aqueous phases. While the polymerisation still gave highly polydispersed reaction mixtures, the batch-to-batch reproducibility was improved with TTAB.

As mentioned above, the toluene fraction of **PBDT-BT** ultimately gave high performance devices of 9.4% PCE. Much like the device optimizations discussed in the first part of this article, several adjustments were made to the device architecture to reach that benchmark. It was decided that inverted device geometry of ITO/ZnO/active layer/MoO_3/Ag would be used instead of the conventional geometry. It has now been demonstrated by a number of research groups that inverted structures give more stable devices and are suited to large area roll-to-roll printing.[3] The polymer:fullerene ratio in the inverted devices was 1:2. The lower molecular weight **PBDT-BT** material from Stille coupling gave comparable performance in conventional and inverted device geometry (Tables 1 and 3). Substituting $PC_{61}BM$ with $PC_{71}BM$ gave expected improvement in device current density (Table 3, entries 1 and 2).

As we have reported previously, the fractionation of the polymeric mixture from Suzuki coupling gave samples with a range of molecular weights from M_n of 19 kg/mol to 136 kg/mol (Table 3). Device performance clearly improved from the DCM fraction (4.6% PCE) to the Tol fraction (8.5%). There is a drop in

performance (6.8%) for the CB fraction primarily as result of poorer processability of the viscous polymer solution. The performance of the prime Tol fraction was further increased to 9.4% with the addition of a fullerene interlayer on top of the ZnO.[1, 34] The atomic force microscopy image of the active layer film with various fractions of the polymer are shown in Figure S13. The surface structure of both films from the CF and Tol fractions indicated favourable nanoscale phase separation with domain size of less than 25 nm whereas the film with the DCM fraction showed increased domain size.

As discussed in the synthesis optimization, it was difficult to reproducibly obtain the prime fraction of **PBDT-BT** in terms of molecular weight range and yield. Table 4 shows the device performance data for toluene fractions obtained from different batches of synthesis. While the molecular weight variation was significant, PCE of close to 9% was commonly recorded for devices containing polymer samples with M_n of ~100 kg/mol.

Conclusion

The full story of the development of a high performance polymer **PBDT-BT** has been summarized in this paper. Starting from the initial design and synthesis of the polymer, the performance of the material was hugely improved through both device and material synthesis optimizations. Power conversion efficiency began at just over 2% for conventional devices to over 9% for devices with inverted geometry. The fact that the optimization process involved several researchers from two institutions over a number of years highlights the difficulties and persistence required to achieve state-of-the-art performance. While it was possible to reproduce the high performance material and devices multiple times, it was difficult to obtain a large enough quantity of prime material for large area device studies due to inherent problems in the polymerization process. In future studies, it will be interesting to examine devices containing **PBDT-BT** with non-fullerene acceptor materials.[35, 36] It is possible that the molecular weight sensitivity of **PBDT-BT**/fullerene devices is less significant with the use of other electron acceptor components.

ASSOCIATED CONTENT

Supporting Information. Experimental procedures on synthesis of the polymers, characterization data and details on device fabrication and testing. This material is available free of charge via the Internet at http://pubs.acs.org.

AUTHOR INFORMATION

Corresponding Author

* Mei.Gao@csiro.au, djjones@unimelb.edu.au, wwh-wong@unimelb.edu.au.

Author Contributions

The manuscript was written through contributions of all authors. / All authors have given approval to the final version of the manuscript.

Funding Sources

Victorian State Government, Australian Renewable Energy Agency, Australian Research Council.

ACKNOWLEDGMENT

This work was made possible by funding to the Victorian Organic Solar Cell Consortium (VICOSC) from the Victorian State Government (DSDBI) and the Australian Renewable Energy Agency (ARENA, Project 2-A018). Current funding from ARENA is administered through the Australian Centre for Advanced Photovoltaics (ACAP). WWHW is supported by an ARC Future Fellowship (FT130100500) and TQ has been supported by fellowships from the CSIRO Office of the Chief Executive and ARENA. This work was performed in part at the Melbourne Centre for Nanofabrication (MCN) in the Victorian Node of the Australian National Fabrication Facility (ANFF). The authors thank Dr Thomas Gengenbach (CSIRO) for the XPS measurements. Responsibility for the views, information, or advice herein is not accepted by the Australian Government.

REFERENCES

1. Subbiah, J.; Purushothaman, B.; Chen, M.; Qin, T.; Gao, M.; Vak, D.; Scholes, F. H.; Chen, X.; Watkins, S. E.; Wilson, G. J.; Holmes, A. B.; Wong, W. W. H.; Jones, D. J., Organic Solar Cells Using a High-Molecular-Weight Benzodithiophene–Benzothiadiazole Copolymer with an Efficiency of 9.4%. *Adv. Mater.* **2015,** 27, 702-705.
2. Yang, J.; Vak, D.; Clark, N.; Subbiah, J.; Wong, W. W. H.; Jones, D. J.; Watkins, S. E.; Wilson, G., Organic Photovoltaic Modules Fabricated by an Industrial Gravure Printing Proofer. *Sol. Energy Mater. Sol. Cells* **2013,** 109, 47-55.
3. Krebs, F. C.; Tromholt, T.; Jorgensen, M., Upscaling of Polymer Solar Cell Fabrication Using Full Roll-to-Roll Processing. *Nanoscale* **2010,** 2, 873-886.
4. Wong, W. W. H.; Banal, J. L.; Geraghty, P. B.; Hong, Q.; Zhang, B.; Holmes, A. B.; Jones, D. J., Organic Photovoltaic Materials — Design, Synthesis and Scale-Up. *Chem. Rec.* **2015,** 15, 1006-1020.
5. Li, Y., Molecular Design of Photovoltaic Materials for Polymer Solar Cells: Toward Suitable Electronic Energy Levels and Broad Absorption. *Acc. Chem. Res.* **2012,** 45, 723-733.
6. Huo, L.; Hou, J., Benzo[1,2-b:4,5-b']dithiophene-based Conjugated Polymers: Band Gap and Energy Level Control and their Application in Polymer Solar Cells. *Polym. Chem.* **2011,** 2, 2453-2461.
7. Zhan, X.; Zhu, D., Conjugated Polymers for High-Efficiency Organic Photovoltaics. *Polym. Chem.* **2010,** 1, 409-419.
8. Bundgaard, E.; Livi, F.; Hagemann, O.; Carlé, J. E.; Helgesen, M.; Heckler, I. M.; Zawacka, N. K.; Angmo, D.; Larsen-Olsen, T. T.; dos Reis Benatto, G. A.; Roth, B.; Madsen, M. V.; Andersson, M. R.; Jørgensen, M.; Søndergaard, R. R.; Krebs, F. C., Matrix Organization and Merit Factor Evaluation as a Method to Address the Challenge of Finding a Polymer Material for Roll Coated Polymer Solar Cells. *Adv. Energy Mater.* **2015,** 5, 1402186.
9. Brabec, C. J.; Gowrisanker, S.; Halls, J. J. M.; Laird, D.; Jia, S. J.; Williams, S. P., Polymer-Fullerene Bulk-Heterojunction Solar Cells. *Adv. Mater.* **2010,** 22, 3839-3856.
10. Heeger, A. J., 25th Anniversary Article: Bulk Heterojunction Solar Cells: Understanding the Mechanism of Operation. *Adv. Mater.* **2014,** 26, 10-28.
11. Lai, T.-H.; Tsang, S.-W.; Manders, J. R.; Chen, S.; So, F., Properties of Interlayer for Organic Photovoltaics. *Mater. Today* **2013,** 16, 424-432.

12. Ratcliff, E. L.; Zacher, B.; Armstrong, N. R., Selective Interlayers and Contacts in Organic Photovoltaic Cells. *J. Phys. Chem. Lett.* **2011,** 2, 1337-1350.
13. Chen, L.-M.; Xu, Z.; Hong, Z.; Yang, Y., Interface Investigation and Engineering - Achieving High Performance Polymer Photovoltaic Devices. *J. Mater. Chem.* **2010,** 20, 2575-2598.
14. Park, J. H.; Lee, T.-W.; Chin, B.-D.; Wang, D. H.; Park, O. O., Roles of Interlayers in Efficient Organic Photovoltaic Devices. *Macromol. Rapid Commun.* **2010,** 31, 2095-2108.
15. Piliego, C.; Holcombe, T. W.; Douglas, J. D.; Woo, C. H.; Beaujuge, P. M.; Fréchet, J. M. J., Synthetic Control of Structural Order in N-Alkylthieno[3,4-c]pyrrole-4,6-dione-Based Polymers for Efficient Solar Cells. *J. Am. Chem. Soc.* **2010,** 132, 7595-7597.
16. Zou, Y.; Najari, A.; Berrouard, P.; Beaupré, S.; Réda Aïch, B.; Tao, Y.; Leclerc, M., A Thieno[3,4-c]pyrrole-4,6-dione-Based Copolymer for Efficient Solar Cells. *J. Am. Chem. Soc.* **2010,** 132, 5330-5331.
17. Zhang, Y.; Hau, S. K.; Yip, H.-L.; Sun, Y.; Acton, O.; Jen, A. K. Y., Efficient Polymer Solar Cells Based on the Copolymers of Benzodithiophene and Thienopyrroledione. *Chem. Mater.* **2010,** 22, 2696-2698.
18. Xiao, Z.; Sun, K.; Subbiah, J.; Qin, T.; Lu, S.; Purushothaman, B.; Jones, D. J.; Holmes, A. B.; Wong, W. W. H., Effect of Molecular Weight on the Properties and Organic Solar Cell Device Performance of a Donor-Acceptor Conjugated Polymer. *Polym. Chem.* **2015,** 6, 2312-2318.
19. Xiao, Z.; Subbiah, J.; Sun, K.; Jones, D. J.; Holmes, A. B.; Wong, W. W. H., Synthesis and photovoltaic properties of thieno[3,2-b]thiophenyl substituted benzo[1,2-b:4,5-b[prime or minute]]dithiophene copolymers. *Polym. Chem.* **2014,** 5, 6710-6717.
20. Xiao, Z.; Subbiah, J.; Sun, K.; Ji, S.; Jones, D. J.; Holmes, A. B.; Wong, W. W. H., Thiazolyl Substituted Benzodithiophene Copolymers: Synthesis, Properties and Photovoltaic Applications. *J. Mater. Chem. C* **2014,** 2, 1306-1313.
21. Wong, W. W. H.; Subbiah, J.; Puniredd, S. R.; Pisula, W.; Jones, D. J.; Holmes, A. B., Benzotriazole-based Donor-Acceptor Conjugated Polymers with a Broad Absorption in the Visible Range. *Polym. Chem.* **2014,** 5, 1258-1263.
22. Qin, T.; Zajaczkowski, W.; Pisula, W.; Baumgarten, M.; Chen, M.; Gao, M.; Wilson, G.; Easton, C. D.; Müllen, K.; Watkins, S. E., Tailored Donor–Acceptor Polymers with an A–D1–A–D2 Structure: Controlling Intermolecular Interactions to Enable Enhanced Polymer Photovoltaic Devices. *J. Am. Chem. Soc.* **2014,** 136, 6049-6055.
23. Kai, Z.; Zhicheng, H.; Chunhui, D.; Lei, Y.; Fei, H.; Yong, C., The Effect of Methanol Treatment on the Performance of Polymer Solar Cells. *Nanotechnology* **2013,** 24, 484003.
24. Chen, Y.; Jiang, Z.; Gao, M.; Watkins, S. E.; Lu, P.; Wang, H.; Chen, X., Efficiency Enhancement for Bulk Heterojunction Photovoltaic Cells via Incorporation of Alcohol Soluble Conjugated Polymer Interlayer. *Appl. Phys. Lett.* **2012,** 100, 203304.
25. Nguyen, W. H.; Bailie, C. D.; Unger, E. L.; McGehee, M. D., Enhancing the Hole-Conductivity of Spiro-OMeTAD without Oxygen or Lithium Salts by Using Spiro(TFSI)2 in Perovskite and Dye-Sensitized Solar Cells. *J. Am. Chem. Soc.* **2014,** 136, 10996-11001.
26. Bach, U.; Lupo, D.; Comte, P.; Moser, J. E.; Weissortel, F.; Salbeck, J.; Spreitzer, H.; Gratzel, M., Solid-State Dye-Sensitized Mesoporous TiO_2 Solar Cells with High Photon-to-Electron Conversion Efficiencies. *Nature* **1998,** 395, 583-585.
27. Grenier, F.; Aïch, B. R.; Lai, Y.-Y.; Guérette, M.; Holmes, A. B.; Tao, Y.; Wong, W. W. H.; Leclerc, M., Electroactive and Photoactive Poly[Isoindigo-alt-EDOT] Synthesized Using Direct (Hetero)Arylation Polymerization in Batch and in Continuous Flow. *Chem. Mater.* **2015,** 27, 2137-2143.
28. Seyler, H.; Subbiah, J.; Jones, D. J.; Holmes, A. B.; Wong, W. W. H., Controlled Synthesis of Poly(3-hexylthiophene) in Continuous Flow. *Beilstein J. Org. Chem.* **2013,** 9, 1492-1500.
29. Seyler, H.; Haid, S.; Kwon, T.-H.; Jones, D. J.; Bäuerle, P.; Holmes, A. B.; Wong, W. W. H., Continuous Flow Synthesis of Organic Electronic Materials – Case Studies in Methodology Translation and Scale-up. *Aust. J. Chem.* **2013,** 66, 151-156.
30. Seyler, H.; Jones, D. J.; Holmes, A. B.; Wong, W. W. H., Continuous Flow Synthesis of Conjugated Polymers. *Chem. Commun.* **2012,** 48, 1598-1600.
31. Seyler, H.; Wong, W. W. H.; Jones, D. J.; Holmes, A. B., Continuous Flow Synthesis of Fullerene Derivatives. *J. Org. Chem.* **2011,** 76, 3551-3556.
32. Bannock, J. H.; Krishnadasan, S. H.; Nightingale, A. M.; Yau, C. P.; Khaw, K.; Burkitt, D.; Halls, J. J. M.; Heeney, M.; de Mello, J. C., Continuous Synthesis of Device-Grade Semiconducting Polymers in Droplet-Based Microreactors. *Adv. Funct. Mater.* **2013,** 23, 2123-2129.
33. Pirotte, G.; Kesters, J.; Verstappen, P.; Govaerts, S.; Manca, J.; Lutsen, L.; Vanderzande, D.; Maes, W., Continuous Flow Polymer Synthesis toward Reproducible Large-Scale Production for Efficient Bulk Heterojunction Organic Solar Cells. *ChemSusChem* **2015**, DOI 10.1002/cssc.201500850.
34. Liao, S.-H.; Jhuo, H.-J.; Cheng, Y.-S.; Chen, S.-A., Fullerene Derivative-Doped Zinc Oxide Nanofilm as the Cathode of Inverted Polymer Solar Cells with Low-Bandgap Polymer (PTB7-Th) for High Performance. *Adv. Mater.* **2013,** 25, 4766-4771.
35. Zhou, N.; Dudnik, A. S.; Li, T. I. N. G.; Manley, E. F.; Aldrich, T. J.; Guo, P.; Liao, H.-C.; Chen, Z.; Chen, L. X.; Chang, R. P. H.; Facchetti, A.; Olvera de la Cruz, M.; Marks, T. J., All-Polymer Solar Cell Performance Optimized via Systematic Molecular Weight Tuning of Both Donor and Acceptor Polymers. *J. Am. Chem. Soc.* **2016,** 138, 1240-1251.
36. Nielsen, C. B.; Holliday, S.; Chen, H.-Y.; Cryer, S. J.; McCulloch, I., Non-Fullerene Electron Acceptors for Use in Organic Solar Cells. *Acc. Chem. Res.* **2015,** 48, 2803-2812.

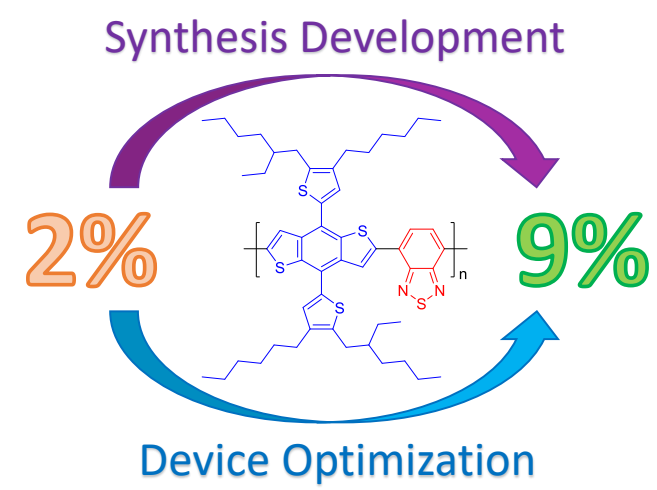
Synthesis Development
2%
9%
Device Optimization